Durable, High-Performance Unitized Reversible Fuel Cells Based on Proton Conductors

Meilin Liu
Georgia Institute of Technology
771 Ferst Drive
Atlanta, GA 30332-0245
Phone: 404-894-6114
Email: meilin.liu@mse.gatech.edu

DOE Manager: David Peterson
Phone: 240-562-1747
Email: David.Peterson@ee.doe.gov

Contract No: DE-EE0008439

Project Start Date: January 1, 2019
Project End Date: December 31, 2021

Overall Objectives

- Develop robust, highly efficient, and economically viable H^+-conducting membrane-based unitized reversible fuel cell (URFC) technology for large-scale co-located energy storage and power generation.
- Gain a profound understanding of the degradation mechanism of cell and stack materials and interfaces, using various in situ, ex situ, and operando measurements guided by theoretical analysis.
- Achieve >70% round-trip efficiency at 1 A cm^{-2} in both operating modes.
- Develop a roll-to-roll manufacturing concept for mass production of URFCs.
- Fabricate prototype large URFCs (6 cm × 6 cm cells with an effective area of 25 cm^2).

Fiscal Year (FY) 2019 Objectives

- Complete literature survey and select state-of-art electrode and electrolyte for URFCs and begin synthesizing materials.
- Fabricate electrode and electrolyte powders of desired properties: homogeneous nanoparticles (50–200 nm diameters) with spherical shape through optimizing the parameters of synthesis.
- Fabricate/microstructure modification of electrode support with diameter of 10 mm: fabricate porous NiO-$BaZr_{0.7}Ce_{0.1}Y_{0.1}Yb_{0.1}O_{3-\delta}$ (BZCYYb) anode support with target porosity of 30% to 40% before reduction.

Technical Barriers

This project addresses the following technical barriers from the Hydrogen Production and Fuel Cells sections of the Fuel Cell Technologies Office Multi-Year Research, Development, and Demonstration Plan[1]:

- Capital cost (Hydrogen Production)
- System efficiency and electricity cost (Hydrogen Production)
- Durability (Fuel Cells)
- Cost (Fuel Cells)
- Performance (Fuel Cells).

Technical Targets

Technical targets for this project in FY 2019 are the following:

- Fabricate electrode and electrolyte powders of desired properties: homogeneous nanoparticles (50–200 nm diameters) with spherical shape.
- Fabricate porous NiO-BZCYYb anode support with diameter of 10 mm and porosity of 30% to 40% before reduction.

FY 2019 Accomplishments

- Completed the literature survey, selected state-of-the-art electrodes and electrolytes for URFCs, and began synthesizing materials.
- Completed the fabrication of electrode and electrolyte powders of desired properties: homogeneous nanoparticles (50–200 nm diameters) with spherical shape through optimizing the parameters of synthesis.

[1] https://www.energy.gov/eere/fuelcells/downloads/fuel-cell-technologies-office-multi-year-research-development-and-22

- Completed fabrication/microstructure modification of electrode support with diameter of 10 mm: fabricated porous NiO-BZCYYb anode support with target porosity of 30% to 40% before reduction.

INTRODUCTION

Solid oxide electrochemical cells have been studied extensively for solid oxide fuel cell applications. However, their potential for large-scale energy storage is yet to be fully explored, especially for electrolysis cells based on proton conductors. Because proton conductors (e.g., BZCYYb) have much higher ionic conductivity than known oxide-ion conductors (e.g., yttria stabilized zirconia), proton conductor-based URFCs can be much more efficient under similar operating conditions. Considering that the electrolysis of water at high temperatures can be highly efficient, the creation of URFCs based on fast proton conductors will dramatically enhance the efficiency of energy storage while reducing the cost and improving the durability and operational life. Our proposed URFC system has the potential to be transformative and disruptive in advancing energy storage and power generation technology. The advantages of our URFC over the conventional oxygen-ion-based cells are compelling: it produces pure/dry H_2 without need for downstream separation/purification, greatly enhances negative electrode durability, and dramatically reduces area specific resistance due to the high conductivity of the electrolyte and highly active electrodes. Furthermore, the scientific knowledge acquired can help to advance other electrochemical technologies based on solid electrolytes such as solid oxide fuel cells and membrane reactors for synthesis of ammonia and other cleaner fuels.

APPROACH

Synthesis and Characterization of Electrodes and Electrolyte Powders

Electrodes ($NdBa_{0.5}Sr_{0.5}Co_{1.5}Fe_{0.5}O_{5+\delta}$ [NBSCF], $PrBa_{0.5}Sr_{0.5}Co_{1.5}Fe_{0.5}O_{5+\delta}$ [PBSCF], and $PrBa_{0.8}Ca_{0.2}Co_2O_{5+\delta}$ [PBCC]) and electrolyte (BZCYYb) powders were synthesized by the combustion, sol-gel, and solid-state reaction methods. Crystal structure and morphology of the synthesized powders were characterized by X-ray diffraction (XRD) and scanning electron microscopy (SEM), respectively. Synthesis parameters (e.g., synthesis method, calcination temperature, heating rate) have been optimized in order to fabricate homogeneous nanoparticles (50–200 nm diameters) with a spherical shape. Electrochemical performance of the air electrodes were measured by electrochemical impedance spectroscopy (EIS) using symmetrical cells.

Fabrication and Characterization of Porous NiO-BZCYYb Anode Support

NiO-BZCYYb anode supports were fabricated by the traditional tape-casting and phase-inversion tape-casting method. The porosity of sintered anode supports was characterized by the Archimedes' method and morphology of the anode was characterized with SEM. In order to get the porous NiO-BZCYYb anode supports with a target porosity of 30% to 40% before reduction, the slurry recipe and sintering temperature were optimized.

RESULTS

Synthesis and Characterization of Electrodes and Electrolyte Powders

In this project, NBSCF, PBSCF, and PBCC double perovskite oxides were fabricated and investigated as air electrodes for URFCs due to their excellent oxygen reduction reaction and/or oxygen evolution reaction activity and durability [1–5]. Powders were synthesized using a combustion method. Stoichiometric amounts of nitrates such as $Nd(NO_3)_3{\cdot}6H_2O$, $Pr(NO_3)_3{\cdot}6H_2O$, $Ba(NO_3)_2$, $Sr(NO_3)_2$, $Co(NO_3)_2{\cdot}6H_2O$, and $Fe(NO_3)_3{\cdot}6H_2O$ were dissolved in distilled water with proper amounts of ethylene glycol and anhydrous citric acid (1:1 ratio). The solutions were heated up to 350°C in air, which resulted in combustion to form fine powders. The resulting powders were then ground and calcined again at various temperatures for 2 hours. As shown in Figure 1a and 1b, the pure layered perovskite structure can be obtained at a sintering temperature higher than 1,000°C for both NBSCF and PBSCF. For PBCC, a pure perovskite structure was formed at a sintering temperature higher than 950°C (see Figure 1c). To further optimize the synthesis conditions, PBCC was synthesized by the sol-gel method. Specifically, stoichiometric amounts of $Pr(NO_3)_3{\cdot}6H_2O$, $Ba(NO_3)_2$, $Ca(NO_3)_2$, and $Co(NO_3)_2{\cdot}6H_2O$ were dissolved in distilled water with proper amounts of citrate acid and

ethylenediaminetetraacetic acid (EDTA) ([glycine]:[EDTA] = 1:1 ratio). The above solutions were mixed and kept at 80°C with continuous stirring. The obtained gel was then dried at 300°C followed by the heat treatment at 1,000°/950°C for 4 h. As shown in Figure 1d and 1e, by decreasing the calcining temperature from 1,000°C to 950°C, the average particle diameter can be reduced from 220 nm to 120 nm. The soft aggregation of PBCC particles shown in Figure 1e can be easily broken into homogeneous spherical nanoparticles (100–200 nm diameters) through a high-energy ball-milling process (see Figure 1f), meeting the requirement of our target.

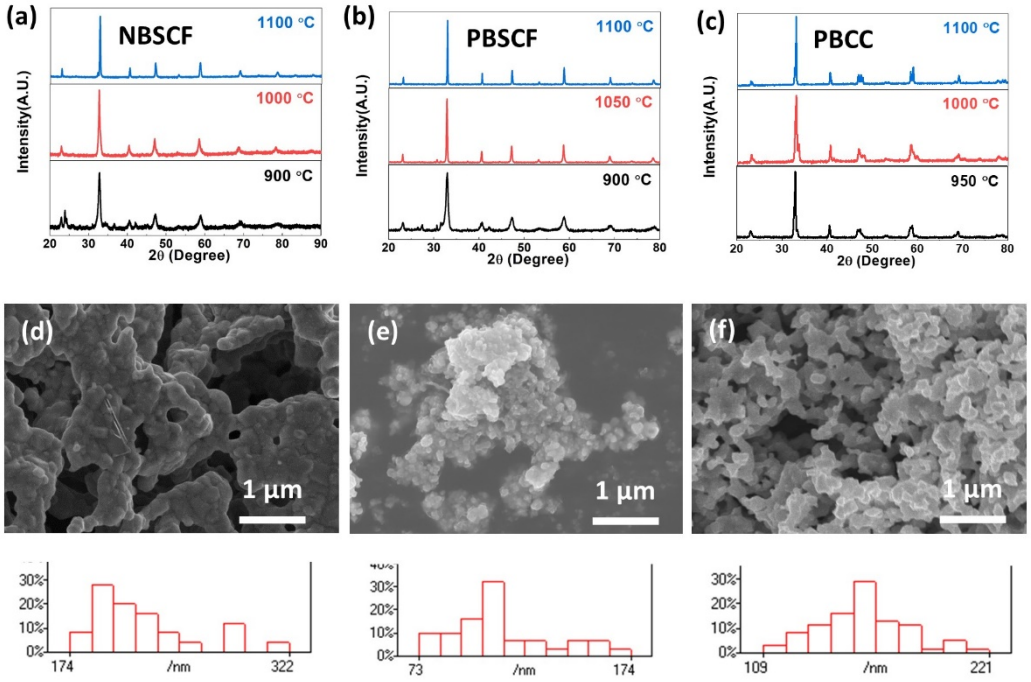

Figure 1. XRD patterns of synthesized (a) NBSCF, (b) PBSCF, and (c) PBCC air electrode powders calcined at various temperatures; SEM images and particle size distributions of synthesized PBCC powders (d) calcined at 1,000°C; (e) calcined at 950°C; and (f) calcined at 950°C and ball-milled.

Similarly, BZCYYb electrolyte powder was synthesized using a sol-gel method. Specifically, stoichiometric amounts of nitrates were used as raw materials and dissolved in distilled water. Citric acid and EDTA were then added in proportion ([CA]:[EDTA] = 1.5:1) serving as chelating and complexing agents, respectively. The above solutions were mixed and kept at 80°C with continuous stirring. The obtained gel was dried at 200°C for 10 h followed by firing at 950°C for 4 h. After firing, the powder was ground using a mortar and pestle. As shown in Figure 2a, spherical BZCYYb particles in the range of 60~150 nm were obtained. The formation of a pure perovskite cubic phase was confirmed by the XRD patterns shown in Figure 2b.

Chemical compatibility between the air electrode and electrolyte materials was evaluated using a composite pellet (weight ratio of the PBSCF/PBCC:BZCYYb = 1:1), which was heat-treated at 1,000°C for 4 h. XRD patterns show the individual phases of the PBSCF/PBCC and BZCYYb without formation of secondary phases (see Figure 2c and 2d), indicating that the PBSCF/PBCC electrode is chemically compatible with BZCYYb under the present processing conditions.

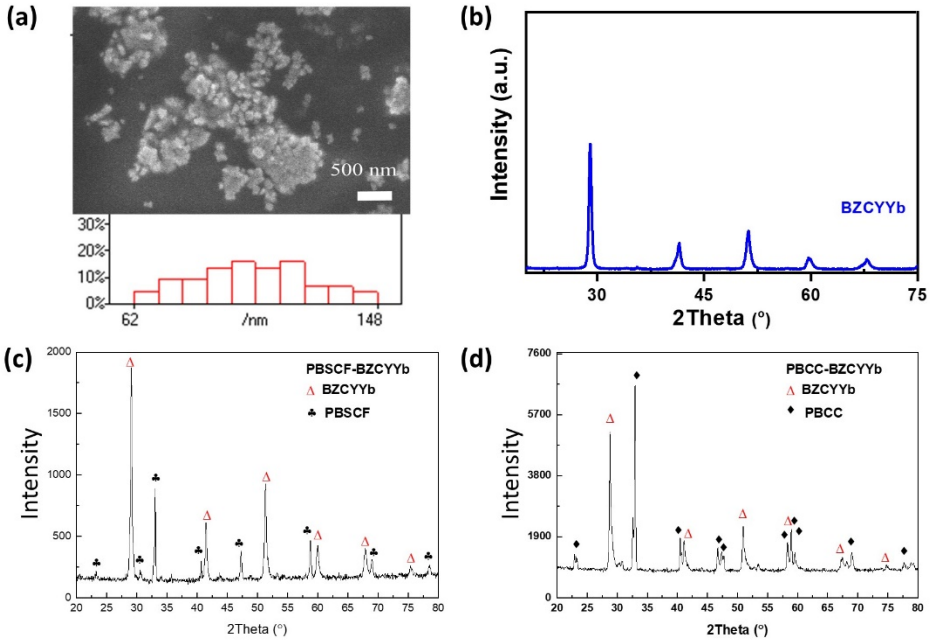

Figure 2. Characterization of the synthesized BZCYYb electrolyte powder: (a) SEM image and particle size distribution; (b) XRD patterns; XRD patterns of the mixed air electrode and electrolyte powders after firing at 1,000 °C for 4 h: (c) PBSCF and BZCYYb composite and (d) PBCC and BZCYYb composite.

As reported, surface coating/modification is an effective approach to enhance the performance of the air electrode [6]. In this project, the surface of PBCC particles was coated with $Gd_{0.2}Ce_{0.8}O_{2-x}$ (GDC) by the Pechini method. First, stoichiometric amounts of $Gd(NO_3)_3$ and $Ce(NO_3)_3$ were dissolved in distilled water. Citric acid and ethylene glycol were then added into the solution with a molar ratio of citric acid:metal ions = 1:1 and ethylene glycol:citric acid = 4:1. The as-synthesized PBCC powder was added into the GDC solution and vigorous stirring was carried out at 70°C for 1 h. The weight ratios of the GDC coating to the PBCC particles were 3:7 and 5:5, respectively. The mixed solution was heated to 250°C to form the precursor powder, followed by calcination at 900°C for 2 h in air. GDC nanoparticles were coated on the surface of the as-synthesized PBCC powder, resulting in enlarged surface area and triple phase boundaries when applied as the electrode (see Figure 3a, 3b, and 3c). To evaluate the electrochemical performance of coated PBCC, symmetrical cells using bare PBCC and coated PBCC were fabricated (950°C, 2 h) and tested. Figure 3d shows a good linearity of the polarization resistance of the electrodes versus the reciprocal temperature over the operating temperatures ranging from 550°C to 750°C, and the activation energies are 1.13, 1.12, and 1.05 eV for the bare PBCC, GDC:PBCC = 3:7, and GDC:PBCC = 5:5 electrodes, respectively. Also shown in Figure 3d is the lower polarization resistance of the GDC-coated PBCC compared to that of the bare PBCC over the entire tested temperature range. To make a clear comparison, EIS spectra of the symmetrical cells are shown in Figure 3e–3i. It is obvious that the decrease in the high- and intermediate-frequency arcs (20 kHz–20 Hz, the first arc) is observed with the GDC coating, which may indicate enhanced kinetics of the charge transfer and mass transfer processes. Based on the preliminary results, we can conclude that the surface coating is an effective method to improve the performance of the PBCC air electrode. Future work will focus on optimization of the composition and morphology of the coating layer.

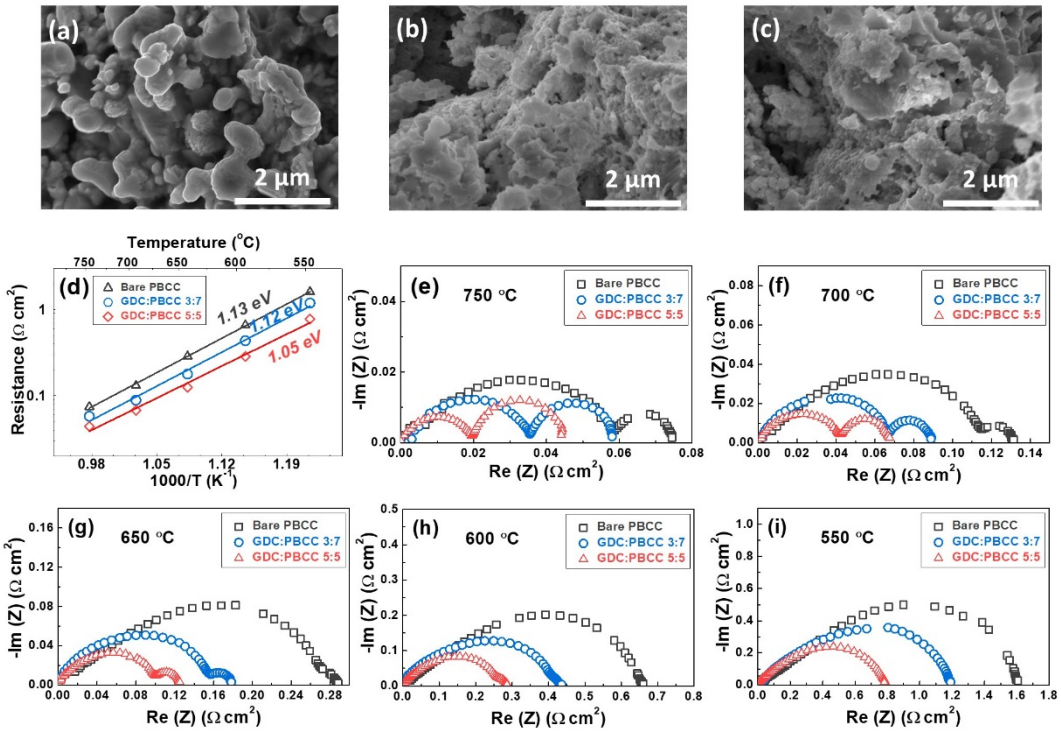

Figure 3. SEM images of the: (a) pure PBCC powder, (b) GDC:PBCC = 3:7 powder, and (c) GDC:PBCC = 5:5 powder; (d) temperature dependence of the polarization resistances of PBCC, GDC:PBCC = 3:7 and GDC:PBCC = 5:5 electrodes; EIS of symmetrical PBCC, GDC:PBCC = 3:7 and GDC:PBCC = 5:5 cells tested at various temperatures: (e) 750°C; (f) 700°C; (g) 650°C; (h) 600°C; and (i) 550°C.

Fabrication and Characterization of Porous NiO-BZCYYb Anode Support

NiO-BZCYYb anode support was fabricated together with the anode functional layer and the electrolyte layer by a tape-casting and co-sintering method. Specifically, the BZCYYb electrolyte powder and the mixture of BZCYYb and NiO powder (NiO:electrolyte powder = 6:4 by weight) were mixed in solvent to form slurries, respectively. The slurry for tape casting was ethanol based and contained a dispersing agent, binder, plasticizer, and other additives, in addition to powder. The electrolyte layer was casted onto the Mylar carrier film first. After drying, the anode functional layer was cast on top of the electrolyte layer, followed by the anode supporting layer. The tri-layer tape was then dried and co-sintered at 1,300°–1,450°C for 5 hours in air. As shown in Figure 4a, porosity of the anode support decreases from 30% at a sintering temperature of 1,300°C to 5% at 1,450°C (see Figure 4b–4e). Also shown in Figure 4a is the increase of the open cell voltage with increasing sintering temperature. To further increase porosity of the anode support, a phase inversion tape-casting method was applied. NiO and BZCYYb powder in the weight ratio of 6:4 were mixed and ball milled for 24 hours using methyl-2-pyrrolidone as the solvent, polyethersulfon as the polymer, and polyvinylpyrrolidone as the binder. After evacuation under vacuum for 30 min, the slurry was tape-casted and then transferred into a water bath for solidification via a phase-inversion process. Then the solidified green tapes were dried and sintered at 1,400°C for 5 h in air. A finger-like porous supporting layer was formed with a high porosity of 35% (see Figure 4f), which meets the requirement of our target (porous NiO-BZCYYb anode support with target porosity of 30% to 40% before reduction).

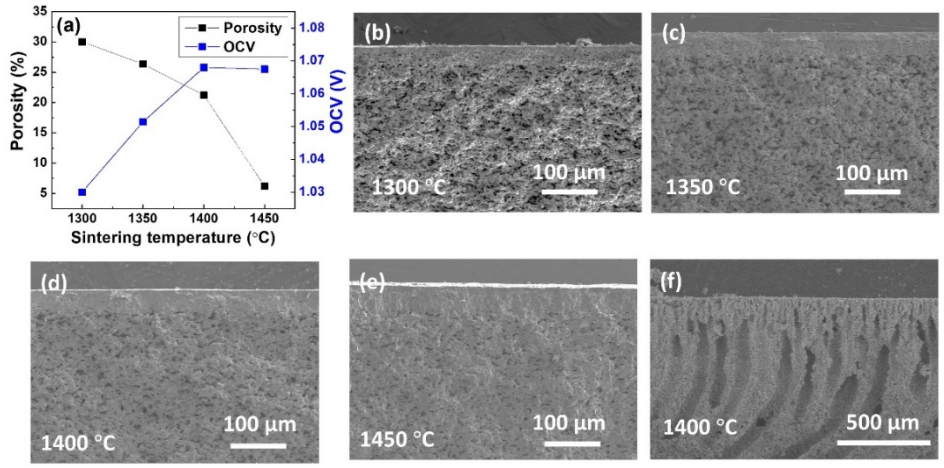

Figure 4. (a) Porosity of NiO-BZCYYb anode supports sintered at various temperatures and open cell voltages of the resulting single cells; (b–e) SEM images of anode supports sintered at various temperatures; (f) SEM image of the anode support fabricated by the phase inversion tape-casting method.

CONCLUSIONS AND UPCOMING ACTIVITIES

In FY 2019, we (1) completed a literature survey and selected state-of-the-art electrodes and electrolyte for URFCs; (2) fabricated electrode and electrolyte powders with particle size of 50–200 nm with a spherical shape through optimizing the synthesis parameters; and (3) completed fabrication and microstructure modification of porous NiO-BZCYYb anode supports with a target porosity of 30% to 40% before reduction. Upcoming work will be the chemical compatibility study of air electrode and oxygen evolution reaction catalysts, and the baseline study of the area specific resistance of the air electrode (0.06 Ω cm^2 under a bias of +0.2 V at 750°C with a durability test of 200 h).

FY 2019 PUBLICATIONS/PRESENTATIONS

1. Yucun Zhou, Yu Chen, Ryan Murphy, and Meilin Liu, "Durable, High-Performance Unitized Reversible Fuel Cells Based on Proton Conductors," poster at the DOE Hydrogen and Fuel Cells Program 2019 Annual Merit Review and Peer Evaluation Meeting, Crystal City, Virginia (April 29–May 1, 2019).

REFERENCES

1. J. Kim, S. Sengodan, G. Kwon, D. Ding, J. Shin, M. Liu, and G. Kim, "Triple-Conducting Layered Perovskites as Cathode Materials for Proton-Conducting Solid Oxide Fuel Cells," *ChemSusChem* 7 (2014): 2811–2815.

2. A. Grimaud, F. Mauvy, J. Bassat, S. Fourcade, L. Rocheron, M. Marrony, and J. Grenier, "Hydration Properties and Rate Determining Steps of the Oxygen Reduction Reaction of Perovskite-Related Oxides as H+-SOFC Cathodes," *Journal of The Electrochemical Society* 159 (2012): B683–B694.

3. C. Duan, R. Kee, H. Zhu, N. Sullivan, L. Zhu, L. Bian, D. Jennings, and R. O'Hayre, "Highly Efficient Reversible Protonic Ceramic Electrochemical Cells for Power Generation and Fuel Production," *Nature Energy* 4 (2019): 230.

4. S. Choi, C.J. Kucharczyk, Y. Liang, X. Zhang, I. Takeuchi, H.-I. Ji, and S.M. Haile, "Exceptional Power Density and Stability at Intermediate Temperatures in Protonic Ceramic Fuel Cells," *Nature Energy* 3 (2018): 202.

5. Y. Chen, S. Yoo, Y. Choi, J.H. Kim, Y. Ding, K. Pei, R. Murphy, Y. Zhang, B. Zhao, and W. Zhang, "A Highly Active, CO_2-Tolerant Electrode for the Oxygen Reduction Reaction," *Energy and Environmental Science* 11 (2018): 2458–2466.

6. J.G. Lee, J.H. Park, and Y.G. Shul, "Tailoring Gadolinium-Doped Ceria-Based Solid Oxide Fuel Cells to Achieve 2 W cm^{-2} at 550 C," *Nature Communications* 5 (2014): 4045.